11th International Symposium on Turbulence and Shear Flow Phenomena (TSFP11)
Southampton, UK, July 30 to August 2, 2019

EXPERIMENTAL INVESTIGATION OF UNSTEADY TURBULENCE USING AN ACTIVE GRID

Abdullah Azzam
Institute for Aerospace Studies
University of Toronto
4925 Dufferin St., North York, ON
abdullah.azzam@mail.utoronto.ca

Philippe Lavoie
Institute for Aerospace Studies
University of Toronto
4925 Dufferin St., North York, ON
lavoie@utias.utoronto.ca

ABSTRACT

Recent studies have reported a departure from Taylor's constant C_ε scaling of the turbulent kinetic energy (TKE) dissipation rate, whereby C_ε was shown to depend on the local Reynolds number Re_λ defined by the Taylor microscale. The present study uses an active grid to produce unsteady flows by approximating step changes and periodic variations of the freestream velocity in an effort to investigate the dependency of the turbulent stochastic fluctuations on the periodic flow component. Results show that the turbulence intensity of the flow depends in the phase-averaged sense on the imposed periodic velocity. The coupling between the turbulent fluctuations and the periodic component is theoretically demonstrated using the TKE budget equation for a periodic flow. Additionally, C_ε is shown to follow the new Re_λ scaling for higher flow frequencies, while being a constant for part of the cycle and following the Re_λ scaling for other parts for low frequencies.

INTRODUCTION

In the well-known Richardson-Kolmogorov cascade, the turbulence is assumed to have reached an asymptotic state where it is at equilibrium. Therefore, the rate at which kinetic energy is supplied by the mean flow is equal to the dissipation rate at the small scales. As a consequence of this equilibrium, the turbulent kinetic energy dissipation rate was shown to scale as

$$\varepsilon = C_\varepsilon \frac{\left(\sqrt{\overline{u'^2}}\right)^3}{L}, \tag{1}$$

by Taylor (1935). In (1), $\sqrt{\overline{u'^2}}$ is the root mean square of the turbulent velocity fluctuations, ε is the mean turbulence kinetic energy dissipation rate, L is the integral length scale, which is considered to be representative of the largest eddies in the flow, while C_ε is a constant.

As reported by Vassilicos (2015), there has been considerable support for the fact that C_ε is a constant through both direct numerical simulations (DNS) and experiments. The findings compiled by Sreenivasan (1984) from the literature and the results of Burattini *et al.* (2005) showed that C_ε asymptoted to a constant value at local Reynolds numbers, $\mathrm{Re}_\lambda \geq 100$ and $\mathrm{Re}_\lambda \geq 60$ respectively, where Re_λ is defined using the Taylor microscale λ, *viz.*

$$\mathrm{Re}_\lambda = \frac{\sqrt{\overline{u'^2}}\lambda}{\nu}. \tag{2}$$

However, a deviation from the constant value of C_ε was first experimentally reported by Seoud & Vassilicos (2007), who showed that along the centerline in the turbulence decay region of fractal grids, C_ε is not constant and scales with Re_λ^{-1}, even though the energy spectra show an extensive region that closely scaled with -5/3. This finding has been readily verified through other experiments involving different flows and grid types. Using PIV to study the wake of square fractal grids, Discetti *et al.* (2013) observed significant variations in the value of C_ε as a function of Re_λ . Similar results were found by Nagata *et al.* (2013) who investigated the turbulent kinetic energy budget by producing cross-sectional profiles of advection, transport, production, diffusion and dissipation terms at various streamwise locations in the wake of fractal grids. Additionally, Isaza *et al.* (2014) found that increasing the inlet Reynolds number for grid-generated turbulence caused an extension of the region within which the new C_ε scaling exists. As a result, Vassilicos (2015) goes on to conclude in his review that the new C_ε scaling was thought to represent a fundamental departure from classical turbulence models.

Recent DNSs of turbulence under the action of a spatially periodic forcing (e.g. Goto & Vassilicos (2016*a*)) reported a similar C_ε scaling given by

$$C_\varepsilon = \frac{\mathrm{Re}_0^{p/2}}{\mathrm{Re}_\lambda^{q}}, \tag{3}$$

where p and q are approximately equal to unity and Re_0 is an inlet Reynolds number that is constant in space and time. However, the results presented by Hearst & Lavoie (2014) and Isaza *et al.* (2014) show that the new scaling (3) does not represent a fundamental violation of (1). Instead, in regions close to the turbulence-generating grids, this new scaling describes a transient process that the turbulence goes through until it reaches equilibrium at locations sufficiently far downstream of the grid, where the dissipation scales according to (1). Nonetheless, the fact that C_ε should follow the same scaling for different flows, in regions where the turbulence has not reached an equilibrium between the large and small scales (the so called non-equilibrium scaling) warrants further investigation.

The aim of this work is to study experimentally the scaling behaviour of turbulent flows that are actively perturbed and hence are not at equilibrium. This study uses an active grid to periodically force the flow and provide a novel insight into the dynamic response of turbulence. This allows the extension of the results from previous DNS studies and the investigation of phase-averaged turbulence quantities to identify any changes in the scaling behaviour.

EXPERIMENTAL SETUP

The active grid used in this study was designed by Hearst & Lavoie (2015), and is shown here in Figure 1. It uses a double-mesh design where half of the wings are mounted onto one plane, and the other half are mounted on the other in an alternating pattern. The streamwise separation between the two meshes is 40 mm. A total of 254 solid square wings are mounted onto rods which are 6.35 mm in diameter and spaced 80 mm apart resulting in a mesh length M = 80 mm. The total number of rods is 50, with 20 horizontal and 30 vertical rods evenly divided between the two meshes. Each rod is connected to an Applied Motion Products STM23S-3RN stepper motor that is driven through serial commands from two RS-485 serial ports.

The active grid was actuated in one of two modes for this study. The first (termed M1) involves the approximation of an instantaneous open/close motion at a specified frequency and wing angle, with stop times enforced when the wings are in an open orientation, similar to Reinke *et al.* (2017). Instantaneous motion was approximated by operating the grid at a speed that is below the operational limit of the stepper motors and that is negligible compared to the speed at which the flow in the tunnel adjusts to the oscillations. The second mode (M2) involves all grid wings completing full rotations at a desired frequency in order to produce a periodic freestream velocity.

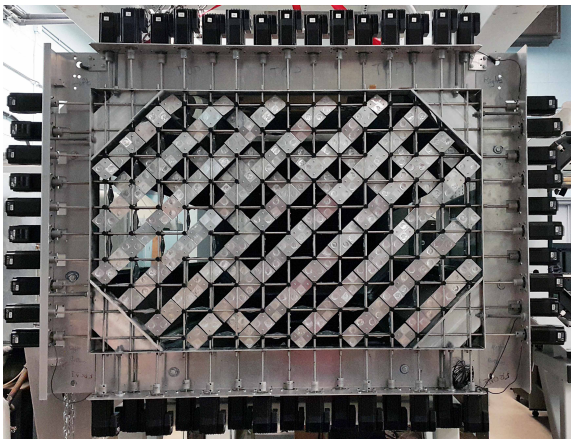

Figure 1: Active grid mounted to test section, stepper motors are shown around the perimeter of the grid in black.

The wind tunnel used to conduct all experiments is the low-speed recirculating wind tunnel in the Flow Control and Experimental Turbulence (FCET) lab at the University of Toronto Institute for Aerospace Studies. The wind tunnel has a hexagonal cross-sectional area that is 1.2 m wide and 0.8 m high. The total test section length is 5 m while the length of the entire wind tunnel circuit is approximately 40 m. Without any grids in place, the maximum reported freestream speed is 40 m/s with a turbulence intensity of 0.08%.

Velocity measurements were taken downstream of the grid at a streamwise distance of $x/M = 26$ using constant temperature anemometry. The anemometers were designed and manufactured at the University of Newcastle (Miller *et al.*, 1987) and an overheat ratio of 1.6 was used. Dantec single-wire probes and probe holders were used, and the hot wires were made in-house with 5μm tungsten wires with a 1 mm sensing length. Calibration of the hot-wires was done *in-situ* with the grid in a fully open configuration. Twelve reference velocities were used for calibration and were obtained using a pitot-static tube placed downstream of the grid. The velocities and hot-wire voltages measured were fit with a fourth-order polynomial.

Data was acquired using a National Instruments (NI) PCIe-6259 data acquisition card and NI BNC-2110 connector block. The filter frequency for the hot-wire signals was determined by conducting sample runs without filter and identifying the position of the noise floor on the power spectral density. Consequently, runs at mean speeds of 4 m/s and 7 m/s were filtered at 2.8 kHz and sampled at 8 kHz, while runs at 10 m/s were filtered at 5.2 kHz and sampled at 12 kHz.

Bias uncertainties were calculated using the methodology presented by Jørgensen (2002). The random uncertainty on the mean flow velocity is given by

$$\delta_{\bar{u}} = 1.96\frac{\sigma_u}{\sqrt{N}}, \tag{4}$$

assuming a 95% confidence interval, where σ_u is the standard deviation of $u(t)$, and N is the number of independent samples in the measurement. Similarly, for phase averaged quantities, random uncertainties are estimated using (4), but with the standard deviation taken over a phase averaged window. Uncertainty on the root mean square (RMS) value of the velocity fluctuations is (Benedict & Gould, 1996)

$$\delta_{u_{RMS}} = 1.96\sqrt{\frac{\overline{u'^2}}{2N}}, \tag{5}$$

which assumes an approximately Gaussian velocity distribution. The bootstrapping algorithm (Benedict & Gould, 1996) was used to calculate uncertainties on other quantities, such as derivatives. Sampling times ranged from 10 to 35 minutes for each test case depending on the desired frequency of the produced flow, where higher frequencies required a shorter time for the statistics to converge. Total

uncertainties typically varied between ±4.5% and ±5.5% on the mean, RMS and peak velocities. At the lower frequencies, the uncertainty gets as high as ±7% due to the lower number of cycles sampled.

Using the triple decomposition method, the measured velocity is expressed as

$$u(t) = \bar{u} + \tilde{u}(t) + u'(t), \tag{6}$$

where $\bar{u}$ is the mean velocity, $\tilde{u}$ represents the periodic component and u' represents the stochastic or turbulent component.

The periodic component $\tilde{u}(t)$ is computed via a phase average *viz.*

$$\tilde{u}(t) = \frac{1}{N_T}\sum_{n=0}^{N_T} u(t+nT), \tag{7}$$

where T represents the period of the signal under consideration, and N_T is the total number of periods within t_s. Finally, the stochastic component is obtained by subtracting the mean and periodic components from the total velocity.

The final result of the triple decomposition process is shown in Figure 2. The amplitude of the velocity signal is determined from $\tilde{u}(t)$, while turbulence statistics can be extracted from $u'(t)$. The dominant flow frequency, which arises due to the rotation of the grid wings at a certain desired frequency, can be determined by examining the power spectral density $E(f)$ of $u(t)$. For instance, varying the grid area at 1 revolution per second causes a peak in the power spectral density (PSD) at 1 Hz, as shown in Figure 3. Furthermore, the triple decomposition method attenuates the dominant flow frequency as also shown in the spectrum of $u'(t)$ in Figure 3.

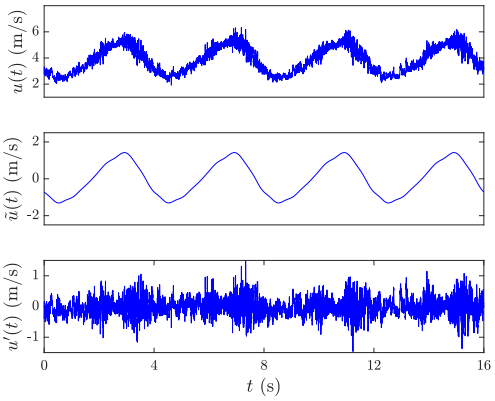

Figure 2: Triple decomposition of velocity signal using M2 into mean, periodic and stochastic components for a mean flow velocity of 4 m/s and a frequency of 0.25 Hz.

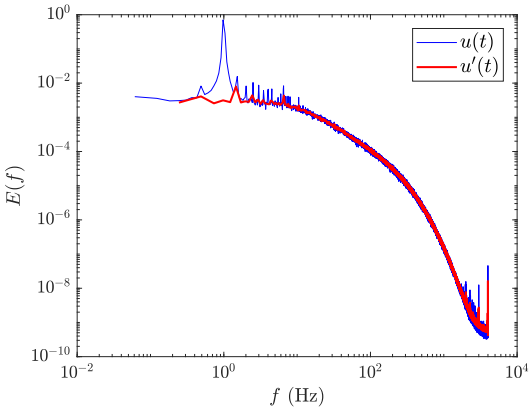

Figure 3: Comparison of power spectral density for $u(t)$ and $u'(t)$ at a mean flow velocity of 4 m/s and a frequency of 1 Hz.

RESULTS

Using the method of triple decomposition discussed earlier, the turbulent kinetic energy (TKE) budget is assessed by substituting this decomposition into the momentum equation. It is assumed that the mean velocity does not vary in time and that the flow is spatially homogeneous, which results in the gradients of the mean and periodic velocities to be equal to zero. The simplified equation is given as

$$\begin{aligned}\left\langle \frac{Dk}{Dt} \right\rangle = &\left\langle -u_i' \frac{1}{\rho}\frac{\partial p}{\partial x_i} - u_j' \frac{\partial\left(\frac{1}{2}u_i'^2\right)}{\partial x_j} \right\rangle - \tilde{u}_j \left\langle \frac{\partial\left(\frac{1}{2}u_i'^2\right)}{\partial x_j} \right\rangle \\ &+ \left\langle \nu \frac{\partial}{\partial x_j}\left(\frac{\partial\left(\frac{1}{2}u_i'^2\right)}{\partial x_j} \right) \right\rangle \\ &+ \left\langle -u_i' \frac{\partial \tilde{u}_i}{\partial t} \right\rangle - \left\langle \nu \left(\frac{\partial u_i'}{\partial x_j} \right)^2 \right\rangle,\end{aligned} \tag{8}$$

where k is the TKE and $\langle\cdot\rangle$ denotes a phase average. In fact, (8) is very similar to the transport equation obtained by Reynolds & Hussain (1972), where the first three terms on the right-hand side denote the transport of TKE due to pressure, the oscillating velocity and viscosity respectively. The last term denotes the dissipation rate of TKE. The main result obtained from (8) is the second to last term which represents the coupling between the periodic and stochastic components of the flow. Therefore, it is thought that this term contributes to the production of TKE by means of the interactions between the turbulent and oscillating components of the velocity. Furthermore, it depends on the frequency and amplitude of the imposed periodic fluctuations, through the time derivative term.

The effect of the grid operating parameters is investigated. Results show a clear modulation of the turbulence intensity during the two modes of operation of the grid, as seen in Figure 4. In M1 at a flow frequency of 0.1 Hz (Figure 4(a)), the rapid flow deceleration between 6.25 s and 7.5 s causes more overshoot in turbulence intensity than the slower acceleration between 1.25 s and 5 s. On the other hand, increasing the flow frequency to 0.5 Hz, causes the flow to approximate a triangular variation in time. As a result, the flow acceleration and deceleration are approximately equal. This is reflected by the similar overshoots in turbulence intensities at 0.75 s and 1.6 s in Figure 4(b). Similar behaviour is observed for the periodic flow velocity generated in M2 in Figures 4(c) and (d). Therefore, this observation provides evidence that the term $\left\langle -u_i' \frac{\partial \tilde{u}_i}{\partial t} \right\rangle$ alters the TKE budget during a flow period.

The effect of the flow frequency in the two modes on

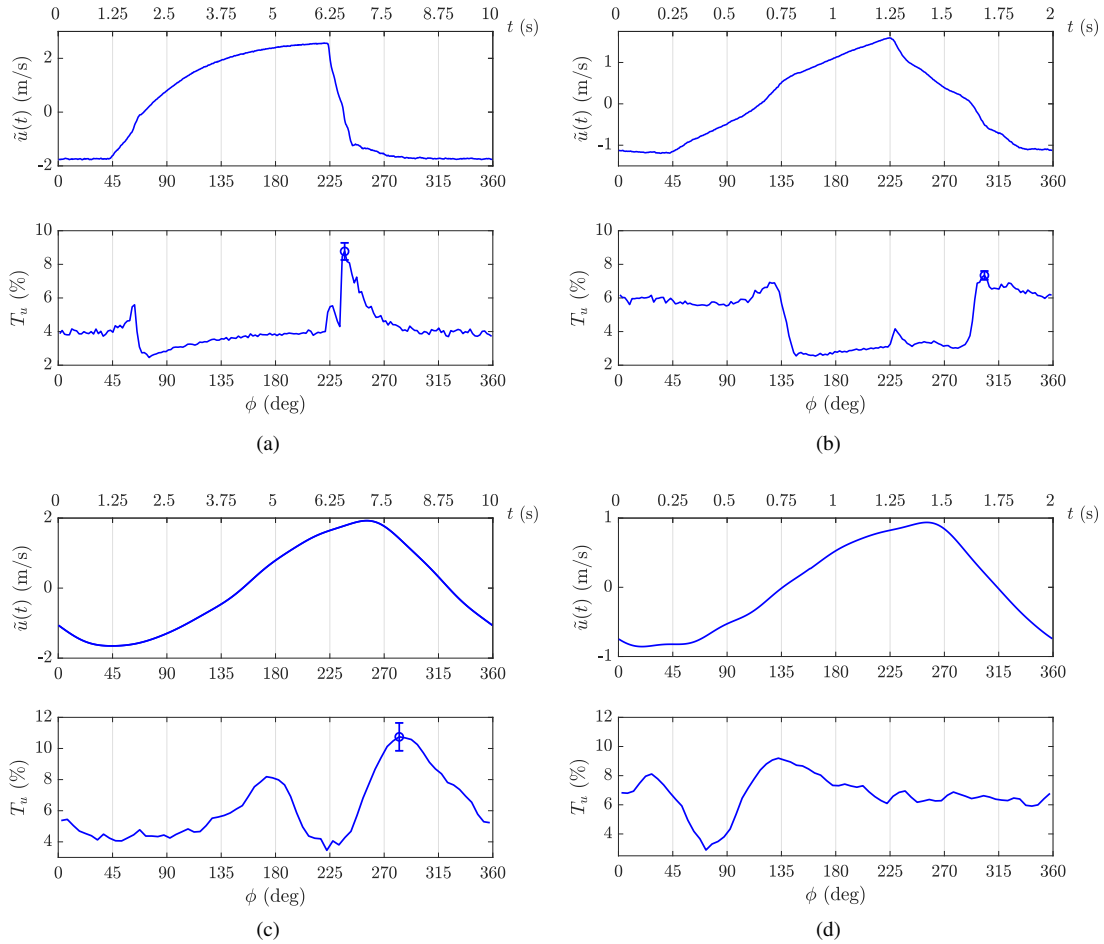

Figure 4: Phase variation of the periodic velocity component and turbulence intensity for (a) M1 at 0.1 Hz, (b) M1 at 0.5 Hz, (c) M2 at 0.1 Hz and (d) M2 at 0.5 Hz at a mean velocity of 4 m/s.

the phase variation of C_ε, which is given by

$$\langle C_\varepsilon \rangle = \frac{\langle \varepsilon \rangle \langle L \rangle}{\langle u' \rangle^3}, \tag{9}$$

is also investigated. In the preceding expression, $\langle \varepsilon \rangle$ is estimated *viz.*

$$\langle \varepsilon \rangle = 15\nu \left\langle \left(\frac{\partial u'}{\partial x} \right)^2 \right\rangle = \frac{15\nu}{\tilde{u}^2} \left\langle \left(\frac{\partial u'}{\partial t} \right)^2 \right\rangle, \tag{10}$$

where Taylor's frozen flow hypothesis is employed in order to estimate $\frac{\partial u'}{\partial x}$. Similarly, the phase averaged integral length scale is calculated using

$$\langle L \rangle = \langle \tilde{u} \rangle \int_0^\infty R_{u'u'}(t) \mathrm{d}t, \tag{11}$$

where $R_{u'u'}(t)$ is the autocorrelation function based on $u'(t)$, with the phase averaged velocity over one period being used as the convective velocity instead of the mean velocity (Kahalerras *et al.*, 1998). Furthermore, the integral time scale, t_x, of $u'(t)$ is assumed to be constant since the majority of the sampled periods exhibited minimal variations in their time scale as shown in Figure 5. Additionally, the time scale obtained for $u'(t)$ is roughly 0.01 s, which is much less than the time scale of the imposed oscillations, and so $u'(t)$ and $\tilde{u}(t)$ are effectively decoupled. The resulting phase variation of C_ε for different flow frequencies is shown in Figure 6. It is apparent that C_ε shows appreciable fluctuations over

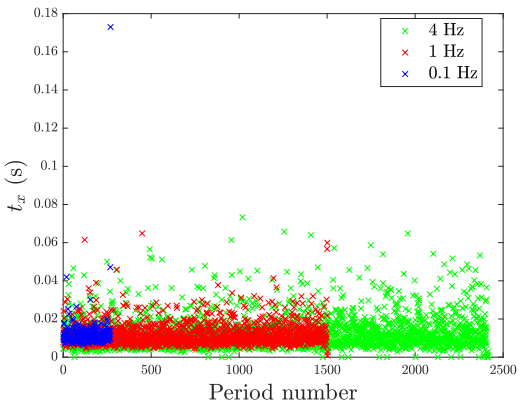

Figure 5: Variation of integral time scale for each flow excitation period at 4 m/s for different flow frequencies.

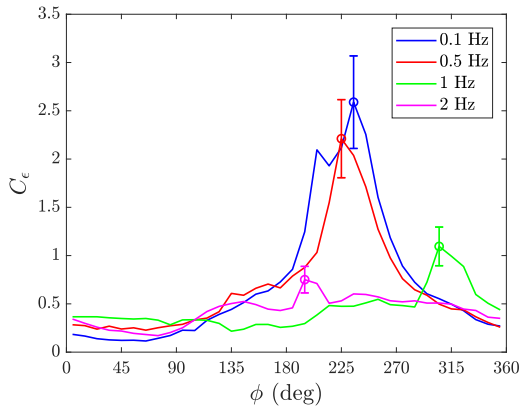

Figure 6: Phase variation of C_ε at 4 m/s for different flow frequencies.

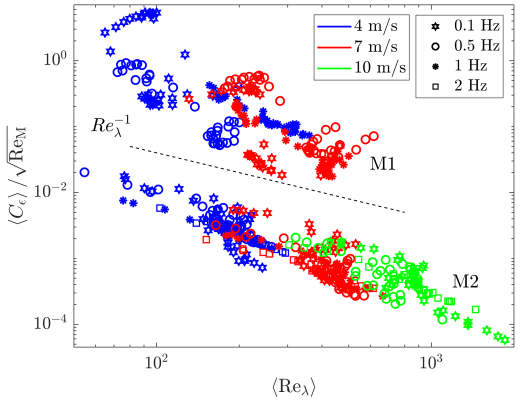

Figure 7: Phase variation of $C_\varepsilon/\sqrt{\mathrm{Re}_M}$ with Re_λ during M1 and M2 for different freestream speeds and flow frequencies. Results from mode M1 are intentionally offset for clarity.

time, which is in agreement with the quasi-periodic fluctuations observed by Goto & Vassilicos (2016*a*) in their DNSs.

Furthermore, based on (3), $C_\varepsilon/\sqrt{\mathrm{Re}_M}$ is plotted against Re_λ in Figure 7, where Re_M is the grid Reynolds number. It can be seen that the data from different cases follow closely the scaling given in (3), which is consistent with the results of Goto & Vassilicos (2016*a*). However, Figure 7 also shows that C_ε exhibits a dependency on the frequency of the oscillating flow. At the lower frequencies, the scaling behaviour varies throughout the duration of one period between the classical Taylor dissipation law (having constant C_ε) and the new scaling identified in (3). This is shown more clearly for the 7 m/s and 0.1 Hz case in Figure 8, where the constant region of C_ε corresponds to regions of fairly constant flow acceleration. Therefore, it is possible here that the lower flow frequencies offer a greater duration for the flow to respond to the imposed oscillations and reach the critical time identified by Goto & Vassilicos (2016*b*) at which C_ε becomes constant, before the flow cycle continues and causes a shift to the Re_λ dependent scaling again.

CONCLUSION

A renewed interest in the scaling of the turbulent kinetic energy (TKE) dissipation rate has been documented recently in literature due to several observations of a departure from the classical constant C_ε scaling first reported by Taylor (1935). Numerous studies have experimentally and numerically shown a dependency of C_ε on the local Reynolds number Re_λ defined on the Taylor microscale. While this does not constitute a fundamental departure from Taylor's classical scaling theory (see Hearst & Lavoie (2014) and Isaza *et al.* (2014)), it nevertheless suggests that the TKE scaling has a consistent transient behaviour that culminates in the steady-state scaling of Taylor (1935).

In this study, an active grid was used to produce unsteady flows approximating step changes in velocity and periodic variations. It was observed that the turbulence intensity of the flow shows considerable modulation over the course of a velocity cycle, whereby higher flow accelerations caused a greater overshoot in turbulence intensity. This was thought to be due to the coupling between the stochastic and periodic components of the flow as demonstrated through the TKE budget equation for periodic flows. C_ε also showed phase-averaged variations which are in agreement with the quasi-periodic fluctuations observed by Goto & Vassilicos (2016*a*). Additionally, a similar dependency of C_ε on Re_λ as that reported in recent literature was clearly illustrated for the higher flow frequencies, while at lower frequencies the C_ε scaling alternated between having a constant value and having a Re_λ dependency.

REFERENCES

Benedict, L. H. & Gould, R. D. 1996 Towards better uncertainty estimates for turbulence statistics. *Exp. Fluids* **22** (2), 129–136.

Burattini, P., Lavoie, P. & Antonia, R. A. 2005 On the normalized turbulent energy dissipation rate. *Phys. Fluids* **17**, 098103.

Discetti, S., Ziskin, I. B., Astarita, T., Adrian, R. J. & Prestridge, K. P. 2013 Piv measurements of anisotropy and inhomogeneity in decaying fractal generated turbulence. *Fluid Dyn. Res.* **45**, 061401.

Goto, S. & Vassilicos, J.C. 2015 Energy dissipation and flux laws for unsteady turbulence. *Phys. Lett. A* **379**, 1144–1148.

Goto, S. & Vassilicos, J.C. 2016*a* Local equilibrium hypothesis and Taylors dissipation law. *Fluid Dyn. Res.* **48**, 021402.

Goto, S. & Vassilicos, J.C. 2016*b* Unsteady turbulence cascades. *Phys. Rev. E* **94**.

Hearst, R. J. & Lavoie, P. 2014 Decay of turbulence generated by a square-fractal-element grid. *J. Fluid Mech.* **741**, 567–584.

Hearst, R. J. & Lavoie, P. 2015 The effect of active grid initial conditions on high Reynolds number turbulence. *Exp. Fluids* **56** (10), 1–20.

Isaza, J. C., Salazar, R. & Warhaft, Z. 2014 On grid-generated turbulence in the near- and far field regions. *J. Fluid Mech.* **753**, 402–426.

Jørgensen, F. E. 2002 How to measure turbulence with hot-wire anemometers - a practical guide. *Dantec Dyn.* .

Kahalerras, H., Malcot, Y., Gagne, Y. & Castaing, B. 1998 Intermittency and Reynolds number. *Phys. Fluids* **10**.

Miller, I. S., Shah, D. A. & Antonia, R. A. 1987 A con-

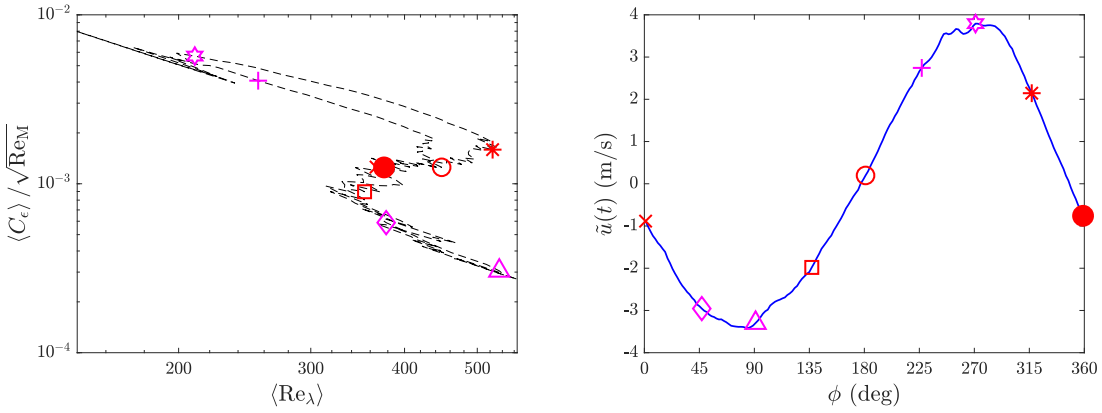

Figure 8: (a) Variation of $C_\varepsilon/\sqrt{\mathrm{Re}_M}$ with Re_λ at 7 m/s and 0.1 Hz with phases identified in accordance with (b), the phase variation of the velocity. Red symbols correspond to regions of constant C_ε, while magenta symbols indicate scaling according to (3).

stant temperature hot-wire anemometer. *J. Phys. E: Sci. Instrum.* **20**, 311–314.

Nagata, K., Sakai, Y., Inaba, T., Suzuki, H., Terashima, O. & Suzuki, H. 2013 Turbulence structure and turbulence kinetic energy transport in multiscale/fractal-generated turbulence. *Phys. Fluids* **25**, 065102.

Reinke, N., Homeyer, T., Hölling, M. & Peinke, J. 2017 Flow modulation by an active grid .

Reynolds, W.C. & Hussain, A.K.M.F. 1972 The mechanics of an organized wave in turbulent shear flow. part 3. theoretical models and comparisons with experiments. *J. Fluid Mech.* **54** (2), 263–288.

Seoud, R. E. & Vassilicos, J. C. 2007 Dissipation and decay of fractal-generated turbulence. *Phys. Fluids* **19**, 105108.

Sreenivasan, K. R. 1984 On the scaling of the turbulence energy dissipation rate. *Phys. Fluids* **27**, 1048.

Taylor, G.I. 1935 Statistical theory of turbulence. *Proc. R. Soc. A, Math. Phys. Eng. Sci.* **151**, 421–444.

Vassilicos, J.C. 2015 Dissipation in turbulent flows. *Annu. Rev. Fluid Mech.* **47**, 97–114.